Optical Absorption Microspectroscopy (μ-OAS) Based on Schwarzschild-Type Cassegrain Optics

Mathieu Chassé,[a] Gérald Lelong,[a] Peter van Nijnatten,[b] Ivo Schoofs,[b] Jürgen de Wolf,[b] Laurence Galoisy,[a] Georges Calas[a]

[a] *Institut de minéralogie, de physique des matériaux et de cosmochimie (IMPMC), Sorbonne Universités, Université Pierre et Marie Curie Paris 06, CNRS UMR 7590, IRD UMR 206, Muséum national d'Histoire naturelle, 4 Place Jussieu, F-75005 Paris, France*
[b] *OMT Solutions BV, High Tech Campus 9, 5656AE Eindhoven, The Netherlands*

A new experimental setup, combining a custom-designed Schwarzschild-type Cassegrain-based microscope and an ultraviolet–visible-near infrared (UV-Vis-NIR) spectrophotometer, has been developed, focusing the light beam down to 20 μm diameter. Optical absorption spectra (in the 300–2500 nm range) have been measured on micrometer-sized natural glass inclusions providing information on iron speciation in magmatic melts. The absence of contribution from the host crystal matrix provides a test of the efficiency of micro-focusing. A microthermometric stage has been adapted on the microscope for measuring optical absorption spectra up to 900 K with application to the thermochromism of minute natural spinel crystals ($MgAl_2O_4$:Fe^{2+},Cr^{3+}). This experimental setup provides an easy and fast way to follow the evolution of spectral properties and color of glasses or crystals with temperature as well as the possibility of measuring spatially resolved optical absorption spectra.

Index Headings: **Optical absorption spectroscopy; OAS; Ultraviolet–visible-near-infrared spectroscopy; UV-Vis-NIR spectroscopy; Microspectrophotometry; Cassegrain microscope; Glass inclusions; Temperature; Spinel.**

INTRODUCTION

Microspectroscopy has been widely developed on various spectroscopic techniques as it brings spatially resolved information. In the case of optical absorption spectroscopy (OAS), even if most efforts have been devoted to microspectroscopy in the IR range,[1,2] common microscopes have been adapted on portable or homemade spectrophotometers in order to give access to the ultraviolet–visible (UV-Vis) range for various applications, e.g., in biology to identify and map deoxyribonucleic acid (DNA) or pigments[3,4] or in the forensic sciences.[5] Ultraviolet–visible microspectroscopy was also used in chemistry and material sciences,[6] but spatial resolution, spectral range, and detection limits were more limited than for standard laboratory spectrophotometers. In earth sciences, in situ high-temperature visible microspectroscopy has been developed to study temperature-induced color change kinetics of volcanic materials.[7] In the specific case of transition elements, an extended wavelength range is required to investigate their spectroscopic properties in microscopic samples, as electronic transitions span a broad range in energy. Recent studies have shown there is interest in developing specific microspectrophotometers or adapting microscopes on laboratory spectrophotometers. For instance, optical absorption microspectroscopy (μ-OAS) in a reflection mode has been developed recently in the range 400–1600 nm.[8] In a transmission mode, some examples of homemade adaptations of optical microscopes on a UV-Vis-NIR spectrophotometer were also reported,[9,10] with the IR and visible regions being measured separately. Then, there is a need for versatile microscopes designed for OAS measurements, working from UV to NIR without chromatic aberrations and allowing spatially resolved OAS, with possible variable temperature or pressure environment.

Here, the development of a versatile microspectrophotometric technique, allowing measurement of optical absorption spectra routinely in a wide range (200–3300 nm) is reported. Unlike a typical optical microscope with an optic based on glass lenses that absorb a large portion of light and exhibit chromatic aberration for such a large wavelength range, this spectrophotometer-fitted microscope features an all-reflective optics, which, besides the UV and visible spectral ranges, ensures the coverage of the entire IR spectral range (~50–10 000 cm^{-1}) with a minimal loss of the signal. The central elements are a pair of reflective condensing objectives with a Schwarzschild-type Cassegrain design (NA = 0.54), which focus the light to samples and then collect the transmitted light from the samples. It allows one to record spatially resolved spectra with a beam diameter ranging from 20 to 120 μm and may be coupled with a heating stage for investigations at variable temperature. This Cassegrain microscope was designed to fit into the sample compartment of a double-beam UV-Vis-NIR spectrophotometer. The efficiency of the setup is illustrated by two μ-OAS studies: (i) spectral measurements of micrometer-sized volcanic glass inclusions trapped in an olivine (Mg_2SiO_4:Fe^{2+}) crystal in order to show the feasibility of measuring μ-optical absorption spectra down to 20 μm and (ii) high-temperature μ-OAS measurements of spinel crystals using a microthermometric stage, in order to test the versatility, the wider wavelength range, and the extended temperature range brought by this setup, in comparison with previous studies.[11]

DESIGN OF THE MICROSCOPE

The experimental setup is based on a custom-designed Cassegrain-type microscope (Fig. 1a), used

Received 2 July 2014; accepted 22 October 2014.
* Author to whom correspondence should be sent. E-mail: mathieu.chasse@impmc.upmc.fr.
DOI: 10.1366/14-07628

0003-7028/15/6904-0457/0

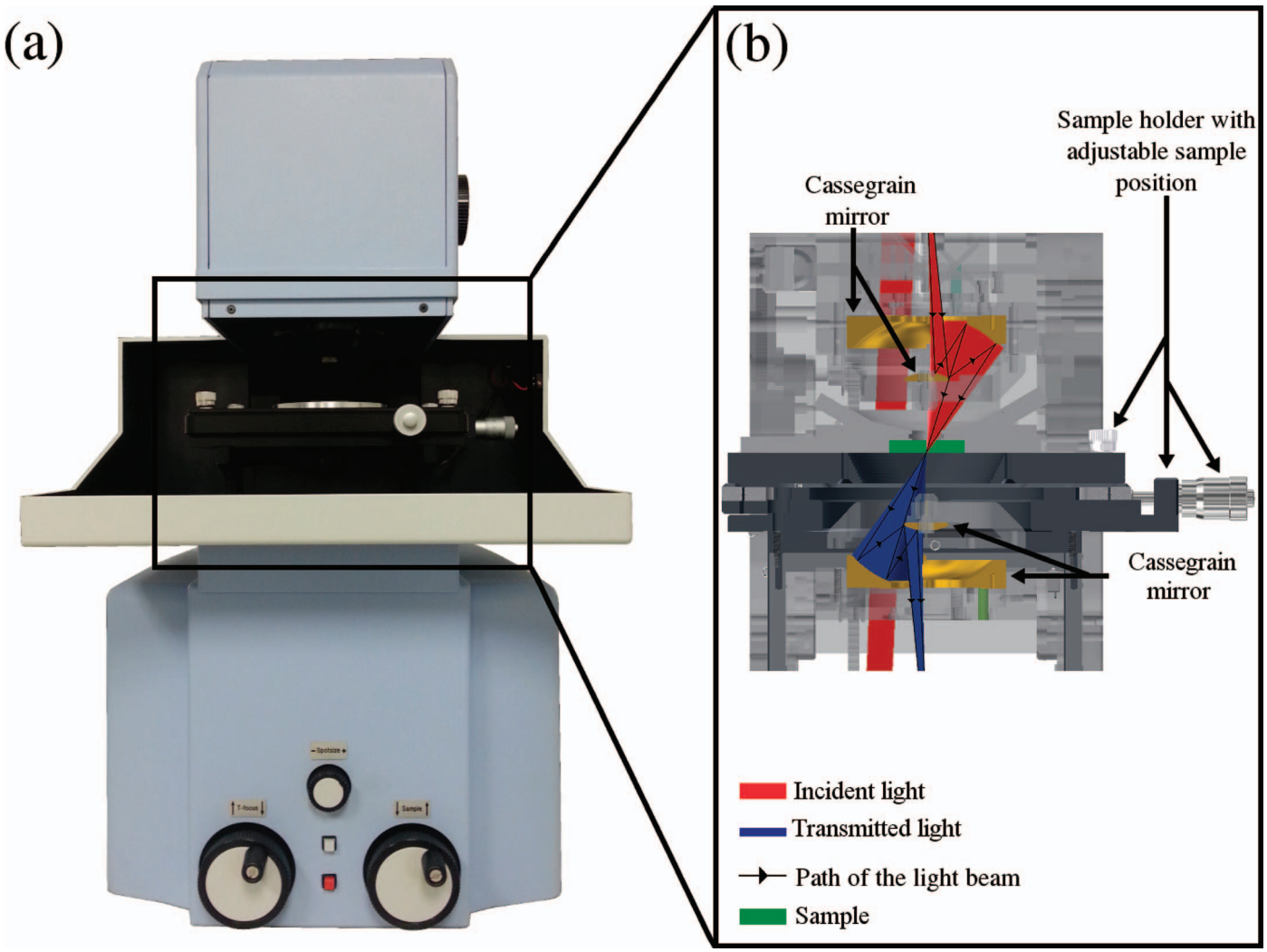

FIG. 1. (**a**) Photograph of the microscope. (**b**) Course of the incident (in red) and transmitted (in blue) light beam through the microscope.

to get spatially resolved optical absorption spectra without any chromatic aberrations, mounted in the sample compartment of a UV-Vis-NIR spectrophotometer (Perkin Elmer Lambda 1050). Measurements are performed using well-defined measurement geometry. The beam is randomly polarized with incident angles evenly distributed in the range 17.3–32.7°. The average angle of incidence is 25.0°. The polarization of the incident beam is random. The microscope allows work in transmission mode with a measurement spot diameter ranging from 20 to 120 μm. The sample beam at the entrance port of the sample compartment of the spectrophotometer (coming from the monochromator) is redirected using flat mirrors towards a spherical mirror just above the upper Schwarzschild objective. The all-reflective optics are coated with UV-enhanced aluminum. Only half of the spherical mirror of the upper Cassegrain objective is employed to focus the beam on the sample (Fig. 1b, red beam). The other half is used in another version of the microscope to recover the beam reflected by the sample. The transmitted light, which is recovered by the lower Cassegrain objective (Fig. 1b, blue light beam), is passed to a spherical mirror and redirected towards the spectrophotometer detector by a series of flat mirrors.

In optical systems, energy conservation is defined by the so-called Helmholtz–Lagrange invariant, which roughly states that an image area multiplied by a solid angle is constant throughout the system, considering only rays that can pass through the system. Light input at the entrance of the microscope is a built-in adjustable aperture which, at maximum opening provides a beam that has the approximate size of 6 × 10 mm (width × height) and a beam solid angle of about 0.0062 sr. The magnification of the microscope is 80 times, and the total solid angle of the beam at the sample is roughly 0.356 sr. Since the beam area at the entrance of the microscope is 80 × 80 = 6400 times larger, the solid angle of the beam accepted at the entrance of the microscope is 6400 times smaller, namely 0.0000556 sr. The maximum energy throughput due to the Helmholtz–Lagrange invariant (not counting reflection losses by the reflecting surfaces in the optical path) is 0.0000556/0.0062 = 0.9%, with a spot size of 75 × 125 μm.

Aluminum coated mirrors have reflection values in the range 85–97%, depending on the wavelength. The minimum reflection of 85% occurs around 830 nm and

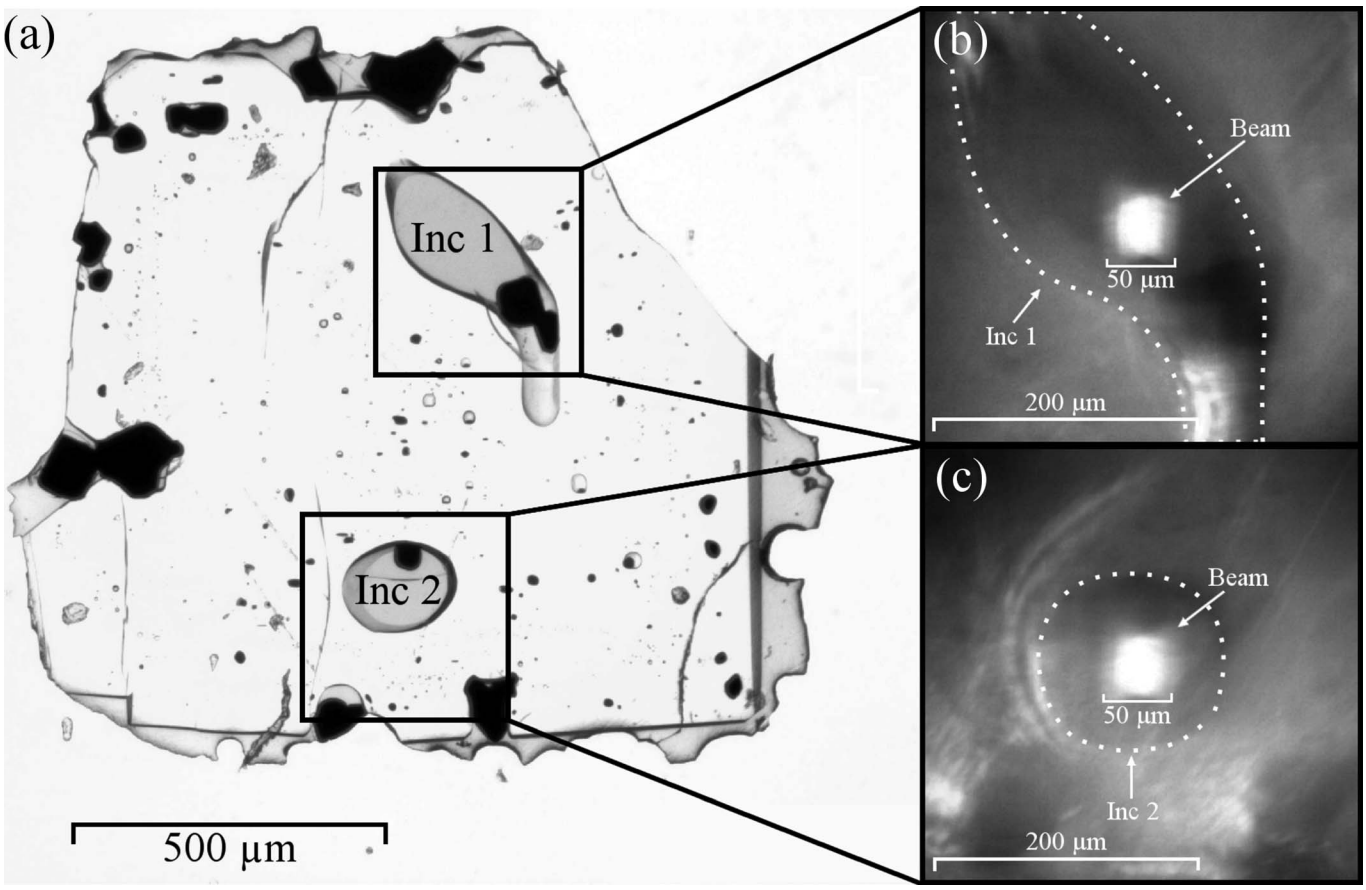

FIG. 2. (**a**) Optical microscope photography of an olivine crystal sample containing two volcanic glass inclusions (Inc 1 and Inc 2). (**b**) and (**c**) Photographs of glass inclusions Inc 1 and Inc 2, respectively, viewed from the camera of the micro-focalized spectrophotometer. Inclusions are highlighted with white-dashed contours; the bright spot evidences the position of the beam inside the inclusions.

at 860 nm, the wavelength where the spectrophotometer has its lowest sensitivity. The beam reflects 14 times on mirrors in the microscope. Taking into account the Helmholtz–Lagrange invariant, the maximum energy throughput (with maximum beam aperture) lies in the range 0.09–0.59% depending on the wavelength. The signal-to-noise (S/N) ratio is improved by beam equalizing optics in the reference beam, using a set of 14 mirrors with the same reflection losses as in the sample beam and a second adjustable aperture.

The microscope is equipped with a charge-coupled device (CCD)-camera and optics providing an image of the sample position through the upper Cassegrain objective. This is used to visualize the beam on the sample during the manual focusing (changing the distance between sample and upper objective). By switching camera optics, a reduced image of the transmitted beam is obtained through the lower Cassegrain objective. This is used to visualize the beam in the focal point of the lower Cassegrain objective during focusing (Fig. 2).

The capabilities of the spectrophotometer are not modified, and spectra can be recorded in the range 200–3000 nm, with a resolution down to 0.1 nm. In the wavelength range 250–2500 nm, the measurement reproducibility is $<$0.1 T% (95% confidence level), and the measurement accuracy is $<$0.5 T%.

The sample chamber of the microscope and the working distance of the Cassegrain objectives (45 mm in total) are large enough to accept a microthermometric stage (Linkam TS1500) that is designed for transmission measurements. By matching the focal points of the two Cassegrain mirrors onto the bottom of the sample through the hole of the ceramic element of the heating stage, optical absorption spectra can be recorded in transmission in the 25–1200 °C temperature range.

EXPERIMENTAL PROCEDURE

A correction procedure has to be applied on the dataset in order to take into account (i) the variations of emissivity between the two lamps of the spectrometer, (ii) the absorption of the aluminum mirrors, (iii) the efficiency of the detectors, and (iv) the sample environment. Two OAS reference spectra are necessary for the correction, one with the light beam going through the sample (I_T) and another without any sample in the light beam (I_0). The optical density (OD) is obtained by the relation

$$\mathrm{OD} = \log_{10}(I_0/I_T) \quad (1)$$

As the emissivity of the furnace cannot be neglected in the IR domain at temperatures above 500 °C, black body emission gives rise to artifacts above this temperature. An additional correction is then necessary. This addi-

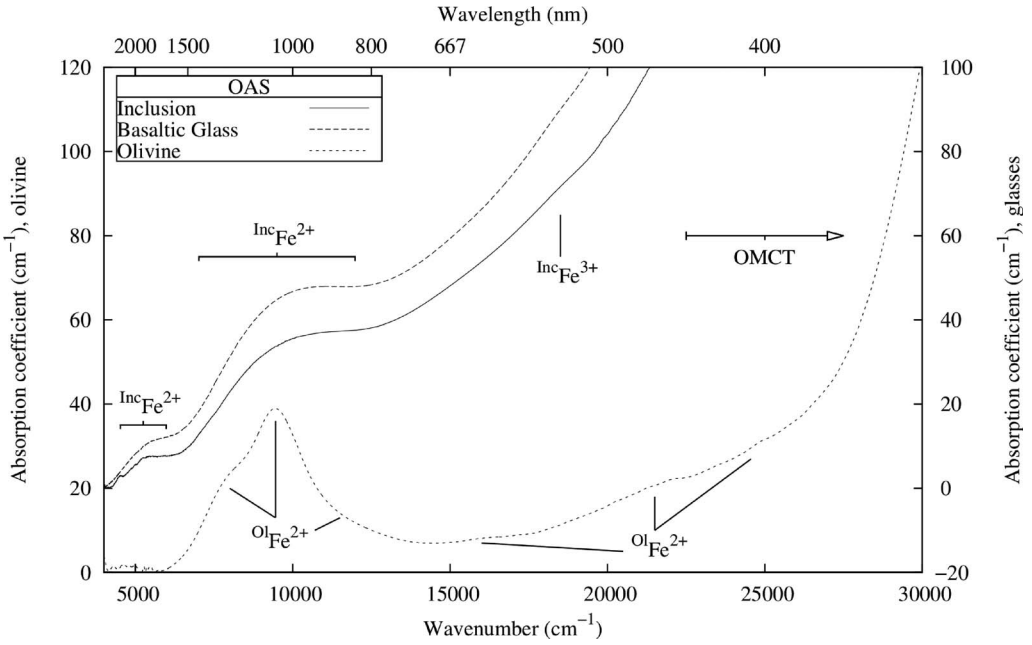

FIG. 3. μ-Optical absorption spectra of glass inclusions Inc 1, of the surrounding olivine crystal and of a basaltic glass in the range 4000–30 000 cm^{-1}. Data are cut at 120 cm^{-1} to better observe the absorption bands in the IR. The positions of the absorption bands originating from the olivine and the inclusions (or basaltic glass) are referred to as ^{Ol}Fe and ^{Inc}Fe, respectively.

tional reference spectrum (I_F) is recorded by masking the incoming light beam. Optical density is deduced as follows

$$OD = \log_{10}\Big(\big(I_0 - I_F\big)/\big(I_T - I_F\big)\Big) \qquad (2)$$

Spectra are then normalized to the thickness of the sample, leading to a linear absorption coefficient.

At high absorbance, an acceptable S/N ratio is obtained for an OD $<$ 1.6, when the microthermometric stage is included. In addition, the low efficiency of the photomultiplier in the NIR region and of the InGaAs detector in the near visible range, associated with the multiple reflections of the beam on the different mirrors, generates noise in the region corresponding to the detector change between PM and the InGaAs detector (around 800 nm). A homemade procedure using Igor Pro 6 has been developed to correct this drawback.

Optical absorption spectra were obtained on double-face polished crystals (about 50 μm thick), which contains glass inclusions. As these inclusions have a size larger than 100 μm, considering the size of the light beam, light may be transmitted through these inclusions without being absorbed by the crystal matrix. The spectra were recorded in the range 2500–330 nm (4000–30 000 cm^{-1}) by using the experimental setup described above, with a 1 nm resolution and a counting time of 0.8 s for each step. The optical density was normalized to the thickness of the sample to obtain the absorption coefficient (cm^{-1}). The same parameters were used to record the optical spectrum of a basaltic glass synthesized from a natural basalt under controlled reducing conditions[12] and used as a reference. These volcanic glass inclusions, as well as the basaltic glass, are Fe-bearing aluminosilicate glasses, whereas the surrounding crystal is an olivine (Mg_2SiO_4:Fe^{2+}). Optical absorption spectra have also been recorded on a natural spinel single crystal ($MgAl_2O_4$), containing Fe^{2+} and Cr^{3+}, which is known for being thermochromic.[9] The crystal has been thinned down to 0.5 mm in order to obtain sufficient transmission for measurement. The measurements were made at controlled temperature between room temperature and 600 °C, with a 100 °C step during heating and cooling.

Color evolution during heating and cooling has been quantified using the $L^*a^*b^*$ coefficients in the colorimetric system defined in 1976 by the International Commission on Illumination (CIE, Commission Internationale d'Eclairage).[13] The determination of the L^*, a^*, and b^* coefficients was made from the transmission spectra obtained at every 5 nm from 380 to 780 nm. A 10° view angle and the CIE standard illuminant D65 (indirect sunlight at 6500 K) were used as measurement conditions. These data are presented in an a^*–b^* diagram.[14] They have also been converted to x and y coefficients to be presented in a chromaticity diagram.

APPLICATIONS

Example of Spatially Resolved Microspectrophotometry on Glass Inclusions. A specific case of microscopic scale investigations is illustrated by natural glass inclusions in minerals, used as a witness of volcanic processes. The study of these small pieces of quenched natural melts has been significantly improved using microspectroscopic techniques such as μ-Raman, μ-Fourier transform infrared (FT-IR),[15] or μ-X-ray absorption techniques,[16] which provide information on the speciation of transition elements in natural magmas. Silicate melt droplets are indeed usually entrapped during crystal growth and preserved upon cooling as

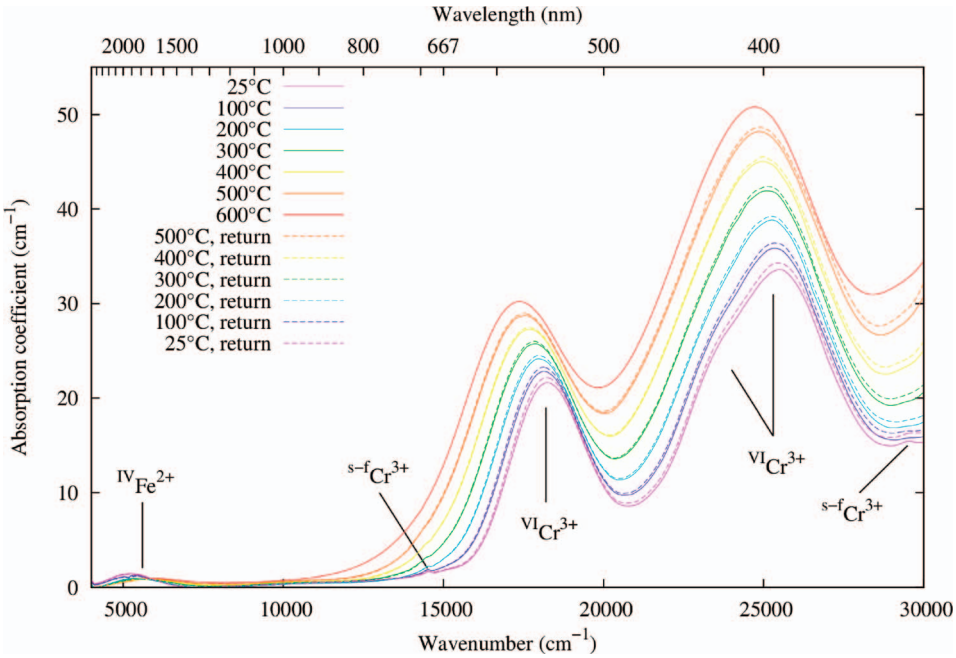

FIG. 4. μ-Optical absorption spectra measured between room temperature and 600 °C on a natural spinel crystal ($MgAl_2O_4$) containing Fe^{2+} and Cr^{3+} impurities. The crystal is 0.5 mm thick. The spectra denoted "return" are recorded during cooling, after heating at 600 °C. The coordination of the cation at the origin of each band is indicated; s-f stands for spin-forbidden transition.

minute glass inclusions. These inclusions record important geochemical parameters, such as primary magma composition, volatile speciation, depth and temperature of magma storage, and nature of open system processes. However, the reduced size of the inclusions, typically around 20 to 100 μm, preclude the use of OAS, despite the information on coordination and oxidation state of transition elements given by this method.[17]

In this case, both glass inclusion and olivine crystal are bearing Fe^{2+} and, to a smaller extent, Fe^{3+} impurities, but the spectral signature of Fe^{2+} being different in OAS between the glass and the crystal, it is possible to probe the spectroscopic features of both the inclusion and the crystalline matrix (olivine, Mg_2SiO_4:Fe^{2+}). The optical absorption spectrum of the inclusion Inc 1, shown in Fig. 3, exhibits in the NIR region a prominent absorption band centered at 9500 cm^{-1} and a shoulder at 5300 cm^{-1}. These absorption bands rise from the presence of Fe^{2+} in basaltic glasses.[18] Similar absorption bands are observed in the basaltic glass of reference. One weak absorption

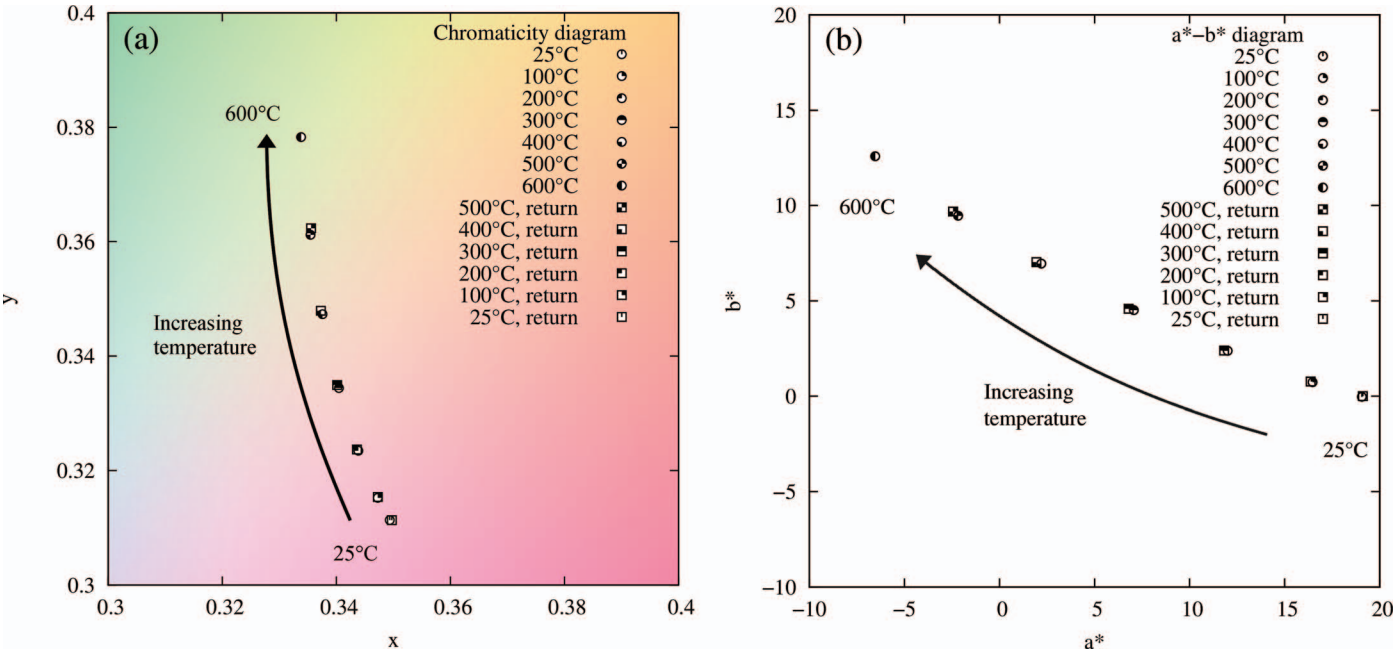

FIG. 5. Evolution of the color of the spinel crystal with increasing temperature from 25 to 600 °C shown (**a**) on a chromaticity diagram and (**b**) on an *a*–b** diagram. The spectra denoted "return" are recorded at the given temperature after heating at 600 °C.

TABLE I. L^*, a^*, and b^* values of the spinel crystal studied at temperatures between 25 and 600 °C. "Return" means that the values are given after heating at 600 °C.

Temperature	25 °C	100 °C	200 °C	300 °C	400 °C	500 °C	600 °C	500 °C, return	400 °C, return	300 °C, return	200 °C, return	100 °C, return	25 °C, return
L^*	61.70	59.76	57.25	54.70	52.36	50.16	48.38	49.96	52.18	54.52	57.03	59.49	61.40
a^*	19.06	16.46	12.00	7.06	2.20	−2.18	−6.53	−2.44	1.94	6.79	11.82	16.37	19.11
b^*	−0.04	0.73	2.38	4.51	6.96	9.46	12.58	9.68	7.04	4.59	2.39	0.77	0.00

band is also observed at 18 500 cm^{-1} and may be interpreted as a spin-forbidden absorption band of Fe^{3+}. In the UV, the absorption edge is associated to the presence of an oxygen-to-iron charge transfer (OMCT). The olivine spectrum (Fig. 3) also shows three intense and rather narrow absorption bands in the NIR region, associated with the presence of Fe^{2+} in the distorted octahedral sites of the olivine structure, M1 and M2.[19] As the position and width of these bands are different between the glass inclusion and the host olivine crystal, the optical absorption spectrum of Inc 1 indicates the spatial selectivity of the experimental setup. Moreover, the weak absorption bands associated with spin-forbidden Fe^{2+} transitions, observable in the visible region in the olivine spectrum, have positions and shapes different from the Fe^{3+} weak absorption band of the inclusion spectrum, confirming the absence of significant contribution from the olivine. The efficiency of micro-focusing, expected from the relative size of the spot and the glass inclusion (Figs. 2b and 2c) is demonstrated over the sample depth by the absence of features arising from the surrounding olivine crystal and confirmed by the similarity between the inclusion spectrum and the spectrum of a basaltic glass.

Microspectrophotometry at High Temperature. The evolution of spectral properties with temperature is illustrated by the optical absorption spectra of a spinel crystal ($MgAl_2O_4$) containing Fe^{2+} and Cr^{3+} impurities (Fig. 4).

Spinel spectra show the absorption bands expected for Fe^{2+} and Cr^{3+} substituted to Mg^{2+} and Al^{3+}, respectively. The absorption band around 18 000 cm^{-1} and the other at 26 000 cm^{-1} with a shoulder at 24 000 cm^{-1} indicate Cr^{3+} transitions in distorted octahedral environment.[9] The absorption band observed at 5000 cm^{-1} is due to tetrahedral Fe^{2+}.[20] Two additional weak and narrow bands, due to Cr^{3+} spin-forbidden transitions are observed at 14 500 and 29 500 cm^{-1}.[9] The possibility to observe these absorption bands evidence the good sensitivity and resolution of the setup.

The thermochromism of the spinel arises from the shift toward the NIR of the two main absorption bands observed in the visible region with increasing temperature. The decreasing energy of the Cr^{3+} absorption bands with increasing temperature is related to an increasing Cr–O distance due to thermal expansion of the crystal structure. The intensity of the absorption of the centrosymmetric site of Cr^{3+} is increasing with increasing temperature due to dynamic removal of the inversion center by vibronic coupling with odd vibrations. As shown in Fig. 5, this shift results in an evolution of the color from pink to green (see also Table I), as observed earlier.[9] This illustrates the possibility of following color changes with temperature using this setup.

The reproducibility of the measurements is illustrated by the superposition of the spectra recorded at the same temperature during heating and during cooling (Fig. 4). This demonstrates the absence of significant oxidation during heating.

CONCLUSION

Measurements of UV-Vis-NIR spectra using a new microspectrophotometer based on a microscope using Schwarzschild-type Cassegrain optics demonstrate its capability for investigating optical absorption spectra at the micrometer scale. This is of special importance for investigating optical absorption spectra over a broad range, without perturbations from chromatic aberrations from a conventional microscope setup. This allows one to investigate spectral properties of transition elements in minute synthetic or natural materials, glassy or crystalline. The versatility of this experimental setup, due to the large size of the sample compartment, will be used for investigating the evolution of optical absorption spectra under high–low temperature and possibly pressure conditions.

ACKNOWLEDGMENTS

We thank Nicole Métrich for providing the natural sample containing the glass inclusions investigated in this study. We also thank the two anonymous reviewers for helping to improve the quality of the manuscript.

1. E.R. Blout, G.R. Bird. "Infrared Microspectroscopy 2". J. Opt. Soc. Am. 1951. 41(8): 547-549.
2. H.J. Humecki. Practical Guide to Infrared Microspectroscopy. New York, NY: Marcel Dekker, 1995.
3. A.W. Coleman, M.J. Maguire, J.R. Coleman. "Mithramycin- and 4′-6-Diamidino-2-Phenylindole (DAPI)-DNA Staining for Fluorescence Microspectrophotometric Measurement of DNA in Nuclei, Plastids, and Virus Particles". J. Histochem. Cytochem. 1981. 29(8): 959-968.
4. V.I. Govardovskii, N. Fyhrquist, T. Reuter, D.G. Kuzmin, K. Donner. "In Search of the Visual Pigment Template". Vis. Neurosci. 2000. 17(4): 509-528.
5. D.R. Cousins, C.R. Platoni, L.W. Russell. "The Use of Microspectrophotometry for the Identification of Pigments in Small Paint Samples". Forensic Sci. Int. 1984. 24(3): 183-196.
6. R. Near, C. Tabor, J. Duan, R. Pachter, M. El-Sayed. "Pronounced Effects of Anisotropy on Plasmonic Properties of Nanorings Fabricated by Electron Beam Lithography". Nano Lett. 2012. 12(4): 2158-2164.
7. Y. Yamanoi, S. Nakashima. "In Situ High-Temperature Visible Microspectroscopy for Volcanic Materials". Appl. Spectrosc. 2005. 59(11): 1415-1419.
8. P. Mouroulis, B. van Gorp, D. Blaney, R.O. Green. "Reflectance Microspectroscopy of Natural Rock Samples in the Visible and Near Infrared". Appl. Spectrosc. 2008. 62(12): 1370-1377.
9. M.N. Taran, K. Langer, A.N. Platonov, V. Indutny. "Optical Absorption Investigation of Cr^{3+} Ion-Bearing Minerals in the

Temperature Range 77–797 K''. Phys. Chem. Miner. 1994. 21(6): 360-372.
10. K. Ullrich, K. Langer, K.D. Becker. ''Temperature Dependence of the Polarized Electronic Absorption Spectra of Olivines. Part I–Fayalite''. Phys. Chem. Miner. 2002. 29(6): 409-419.
11. L. Kido, M. Mueller, C. Ruessel. ''Redox Reactions During Temperature Change in Soda-Lime-Silicate Melts Doped with Copper and Iron or Copper and Manganese''. J. Non-Cryst. Solids. 2006. 352(38): 4062-4068.
12. M. Bonnin-Mosbah, A.S. Simionovici, N. Métrich, J.-P. Duraud, D. Massare, P. Dillmann. ''Iron Oxidation States in Silicate Glass Fragments and Glass Inclusions with a XANES Micro-Probe''. J. Non-Cryst. Solids. 2001. 288(1-3): 103-113.
13. G. Wyszecki, W.S. Stiles. Color Science: Concepts and Methods, Quantitative Data and Formulae. Chichester, UK: John Wiley and Sons, 2008. 2nd ed.
14. C. Onga, S. Nakashima. ''Darkfield Reflection Visible Microspectroscopy Equipped with a Color Mapping System of a Brown Altered Granite''. Appl. Spectrosc. 2014. 68(7): 740-748.
15. N. Métrich, P.J. Wallace. ''Volatile Abundances in Basaltic Magmas and Their Degassing Paths Tracked by Melt Inclusions''. Rev. Mineral. Geochem. 2008. 69(1): 363-402.
16. M. Bonnin-Mosbah, N. Métrich, J. Susini, M. Salome, D. Massare, B. Menez. ''Micro X-Ray Absorption Near Edge Structure at the Sulfur and Iron K-Edges in Natural Silicate Glasses''. Spectrochim. Acta, Part B. 2002. 57(4): 711-725.
17. G.R. Rossman. ''Optical Spectroscopy''. Rev. Mineral. Geochem. 2014. 78(1): 371-398.
18. W.E. Jackson, F. Farges, M. Yeager, P.A. Mabrouk, S. Rossano, G.A. Waychunas, et al. ''Multi-Spectroscopic Study of Fe(II) in Silicate Glasses: Implications for the Coordination Environment of Fe(II) in Silicate Melts''. Geochim. Cosmochim. Acta. 2005. 69(17): 4315-4332.
19. R.G. Burns. Mineralogical Applications of Crystal Field Theory. Cambridge, UK: Cambridge University Press, 1993. 2nd ed.
20. G.R. Rossman, M.N. Taran. ''Spectroscopic Standards for Four- and Fivefold-Coordinated Fe^{2+} in Oxygen-Based Minerals''. Am. Mineral. 2001. 86(7-8): 896-903.